AIAA JOURNAL
Vol. 36, No. 5, May 1998

Development of an Improved Kirchhoff Method for Jet Aeroacoustics

Anthony R. Pilon*
University of Minnesota, Minneapolis, Minnesota 55455
and
Anastasios S. Lyrintzis†
Purdue University, West Lafayette, Indiana 47907

Research in the development of an improved Kirchhoff method is described. The Kirchhoff method is a means of evaluating radiated sound from flow acoustic quantities on a computational surface. The linear, homogeneous wave equation is assumed to be valid in the propagation region, outside this surface (the Kirchhoff surface). The surface quantities are generally obtained from a computational fluid dynamics (CFD) calculation of the acoustic near field. We outline the development of a Kirchhoff method for use when the linear, homogeneous wave equation is not valid in a portion of the region outside of the Kirchhoff surface. The new method is derived through the use of a permeable-surface formulation of the Ffowcs Williams–Hawkings equation. This modified integral equation allows the Kirchhoff methodology to be employed in problems with large, noncompact source regions that extend beyond the limits of the CFD calculation. Test calculations are presented in an attempt to validate the method for use in jet aeroacoustics studies. However, the method is presented in a manner to make it easily applicable in cases where Kirchhoff methods have been used in the past.

Nomenclature

a	= sound speed
g_{ij}	= metric tensor components
$H(f)$	= Heaviside function
L_k, R_k	= Kirchhoff surface dimensions
M	= surface Mach number
$\hat{n}$	= unit surface normal vector
p, ρ	= fluid pressure and density
$\boldsymbol{r}$, $\hat{r}$	= radiation and unit radiation vectors
S, $\mathrm{d}S$	= Kirchhoff surface area
T_{ij}	= Lighthill stress tensor
u^i	= Kirchhoff surface local coordinates
u_i	= fluid velocity
v_i	= Kirchhoff surface velocity
(x_i, t)	= observer coordinates and time
(y_i, τ)	= source coordinates and time
$\delta(f)$	= Dirac delta function
θ	= emission angle
κ	= complex wave number
λ	= acoustic wavelength
σ_{ij}	= viscous stress tensor
ϕ	= wave variable, $(a_0^2\rho')$
ω	= angular frequency
$\Box$	= D'Alembertian wave operator

Subscripts

n	= surface normal direction
r	= radiation direction
o	= ambient conditions

Superscript

$'$	= disturbance quantity

Received July 11, 1996; revision received Feb. 25, 1997; accepted for publication Jan. 13, 1998.

*Graduate Research Assistant, Department of Aerospace Engineering and Mechanics; currently Research Associate, Department of Aerospace Engineering, Pennsylvania State University, University Park, PA 16802. Member AIAA.

†Associate Professor, School of Aeronautics and Astronautics. Associate Fellow AIAA.

I. Introduction

THE use of Kirchhoff's integral equation[1] as a tool for numerical acoustic prediction has increased recently.[2] The Kirchhoff method is a means of extending near-field acoustic data, through the numerical evaluation of surface integrals, to the acoustic far field. The near-field acoustic data are usually obtained through the use of a computational fluid dynamics (CFD) code. This method is attractive because it utilizes surface integrals over a source region to determine far-field acoustics. Acoustic analogy methods require the evaluation of volume integrals, and so there is a large savings in required computational resources. Additionally, the Kirchhoff method does not suffer the dissipation and dispersion errors found when the midfield and far-field sounds are directly calculated with an algorithm similar to those used in CFD studies.

There are difficulties with using the Kirchhoff and related methods for some aeroacoustic problems. For an accurate prediction, the Kirchhoff control surface must completely enclose the aerodynamic source region. This may be difficult or impossible to accomplish if the source region is large. The validity of this method is also dependent on the Kirchhoff surface being placed in a region where the linear wave equation is valid. Difficulties meeting these criteria frequently arise in jet acoustics and similar studies.

This paper outlines the development of improvements to the Kirchhoff method for use in aeroacoustic calculations. The improvements arise from an analysis of a permeable-surface form of the Ffowcs Williams–Hawkings equation.[3] The formulation of these improvements was outlined by Pilon and Lyrintzis.[4,5] The results are based on the developments of Farassat and Myers.[6] Recently, Di Francescantonio[7] and Brentner and Farassat[8] presented permeable-surface extensions of the Ffowcs Williams–Hawkings equation for nondeforming, moving surfaces and showed the similarities to the Kirchhoff integral equation. The improvements presented here are similar in nature to those presented by these authors but are intended for use with existing Kirchhoff methods. Some validation calculations, which are suitable for jet noise studies, are presented as well.

II. Modified Kirchhoff Formulation

Crighton et al.,[9] following the development of Lighthill's equation[10] using generalized function theory,[11,12] presented a form of the Ffowcs Williams–Hawkings equation[3] for an arbitrarily moving, permeable, deformable surface. The surface may be a real, solid surface, possibly with blowing or suction, or a permeable computational

control surface. The mathematics are identical. This formulation may be written

$$\Box^2[\phi H(f)] = \frac{1}{a_o^2}\frac{\partial^2}{\partial t^2}[\phi H(f)] - \frac{\partial^2}{\partial x_i^2}[\phi H(f)]$$

$$= \frac{\partial^2}{\partial x_i \partial x_j}[T_{ij}H(f)] - \frac{\partial}{\partial x_i}\{[(p-p_o)\delta_{ij} - \sigma_{ij}]\hat{n}_j\delta(f)\}$$

$$+ \frac{\partial}{\partial t}[\rho_o v_n \delta(f)] + \frac{\partial}{\partial t}[\rho(u_n - v_n)\delta(f)]$$

$$- \frac{\partial}{\partial x_i}[\rho u_i(u_n - v_n)\delta(f)] \tag{1}$$

The surface is defined by $f(\boldsymbol{x}, t) = 0$ such that $f > 0$ in the fluid outside the surface and $f < 0$ inside the surface. Then the unit outward normal to the surface can be defined as $\hat{\boldsymbol{n}} = \nabla f$. Also, $\phi = a_o^2(\rho - \rho_o)$, $\rho' = \rho - \rho_o$, $u_n = u_i\hat{n}_i$, $v_n = v_i\hat{n}_i$, and Lighthill's stress tensor is

$$T_{ij} = \rho u_i u_j - \sigma_{ij} + \left[(p - p_o) - a_o^2\rho'\right]\delta_{ij}$$

The first three terms on the right-hand side of Eq. (1) compose the original Ffowcs Williams–Hawkings equation,[3] whereas the last two terms are the contributions to the radiated sound caused by the permeability of the surface. Note that in the linear acoustic radiation field $p' = p - p_o = \phi$, so that the left-hand side of Eq. (1) can be written $\Box^2 p'$ if desired. This equation can be evaluated to form an integral equation for numerical prediction of aerodynamically generated noise.[8]

At this point it is desirable to rewrite Eq. (1) in a different form. The new form will produce an integral formulation equivalent to the Kirchhoff integral equation, provided the surface remains permeable and the disturbance density ϕ is used as the dependent variable.

To derive an equivalent expression, first note that

$$-\frac{\partial}{\partial x_i}\{[(p-p_o)\delta_{ij} - \sigma_{ij}]\hat{n}_j\delta(f)\} - \frac{\partial}{\partial x_i}[\rho u_i u_n \delta(f)]$$

$$= -\frac{\partial}{\partial x_i}[T_{ij}\hat{n}_j\delta(f)] - \frac{\partial}{\partial x_i}\left[a_o^2\rho'\hat{n}_i\delta(f)\right]$$

$$\frac{\partial}{\partial t}[\rho_o v_n\delta(f)] + \frac{\partial}{\partial t}[-\rho v_n\delta(f)] = -\frac{\partial}{\partial t}[\rho' v_n\delta(f)]$$

Equation (1) can then be recast as

$$\Box^2[\phi H(f)] = \frac{\partial^2}{\partial x_i \partial x_j}[T_{ij}H(f)] - \frac{\partial}{\partial x_i}[T_{ij}\hat{n}_j\delta(f)]$$

$$- \frac{\partial}{\partial x_i}\left[a_o^2\rho'\hat{n}_i\delta(f)\right] - \frac{\partial}{\partial t}[\rho' v_n\delta(f)] + \frac{\partial}{\partial x_i}[\rho u_i v_n\delta(f)]$$

$$+ \frac{\partial}{\partial t}[\rho u_n\delta(f)] \tag{2}$$

Using the chain rule allows the last two terms to be written as

$$\frac{\partial}{\partial x_i}[\rho u_i v_n\delta(f)] + \frac{\partial}{\partial t}[\rho u_n\delta(f)] = \frac{\partial}{\partial x_i}[\rho u_i]v_n\delta(f)$$

$$+ \rho u_i\frac{\partial}{\partial x_i}[v_n\delta(f)] + \frac{\partial}{\partial t}[\rho u_i]\hat{n}_i\delta(f) + \rho u_i\frac{\partial}{\partial t}[\hat{n}_i\delta(f)]$$

Note also that

$$\rho u_i\frac{\partial}{\partial x_i}[v_n\delta(f)] + \rho u_i\frac{\partial}{\partial t}[\hat{n}_i\delta(f)] = -\rho u_i\left\{\frac{\partial}{\partial x_i}\left[\frac{\partial f}{\partial t}\delta(f)\right]\right.$$

$$\left. - \frac{\partial}{\partial t}\left[\frac{\partial f}{\partial x_i}\delta(f)\right]\right\} = 0$$

and from the conservation equations,

$$\frac{\partial}{\partial x_i}[\rho u_i]v_n\delta(f) = -\frac{\partial\rho'}{\partial t}v_n\delta(f) \tag{3}$$

$$\frac{\partial}{\partial t}[\rho u_i]\hat{n}_i\delta(f) = -\frac{\partial}{\partial x_j}[(p-p_o)\delta_{ij} - \sigma_{ij}]\hat{n}_i\delta(f)$$

$$- \frac{\partial}{\partial x_j}[\rho u_i u_j]\hat{n}_i\delta(f) = -\frac{\partial T_{ij}}{\partial x_j}\hat{n}_i\delta(f) - a_o^2\frac{\partial\rho'}{\partial n}\delta(f) \tag{4}$$

The combination of Eq. (2) with Eqs. (3) and (4) leads to

$$\Box^2[\phi H(f)] = \frac{\partial^2}{\partial x_i\partial x_j}[T_{ij}H(f)] - \frac{\partial}{\partial x_i}[T_{ij}\hat{n}_j\delta(f)] - \frac{\partial T_{ij}}{\partial x_j}\hat{n}_i\delta(f)$$

$$- \left(\frac{\partial\phi}{\partial n} + \frac{1}{a_o}M_n\frac{\partial\phi}{\partial t_x}\right)\delta(f) - \frac{1}{a_o}\frac{\partial}{\partial t}[M_n\phi\delta(f)] - \frac{\partial}{\partial x_i}[\phi\hat{n}_i\delta(f)] \tag{5}$$

where $M_n = v_n/a_o$. The subscript x on the time derivative denotes derivation with respect to time, holding the observer coordinates fixed. This equation was used by the authors to derive a surface integral equation that they referred to as the modified Kirchhoff integral.[4,5] However, further simplification, which was not presented in those papers, is possible. This simplification becomes evident if we note that

$$\frac{\partial^2}{\partial x_i\partial x_j}[T_{ij}H(f)] = \frac{\partial^2 T_{ij}}{\partial x_i\partial x_j}H(f) + \frac{\partial}{\partial x_i}[T_{ij}\hat{n}_j\delta(f)] + \frac{\partial T_{ij}}{\partial x_j}\hat{n}_i\delta(f) \tag{6}$$

Thus, Eq. (5) becomes

$$\Box^2[\phi H(f)] = -\left(\frac{\partial\phi}{\partial n} + \frac{1}{a_o}M_n\frac{\partial\phi}{\partial t_x}\right)\delta(f) - \frac{1}{a_o}\frac{\partial}{\partial t}[M_n\phi\delta(f)]$$

$$- \frac{\partial}{\partial x_i}[\phi\hat{n}_i\delta(f)] + \frac{\partial^2 T_{ij}}{\partial x_i\partial x_j}H(f) \tag{7}$$

[It is possible to derive Eq. (7) directly from the continuity and momentum equations. However, the authors feel that showing the steps actually performed in the development of the current formulation will help show the relationship between the Ffowcs Williams–Hawkings and Kirchhoff formulations.] This equation can now be evaluated to produce a Kirchhoff integral formulation. The derivation here follows that of Farassat and Myers.[6] The free-space Green's function [$G = \delta(g)/4\pi r$; $g = \tau - t + r/a_o$] is used to solve Eq. (7):

$$4\pi\phi(\boldsymbol{x}, t) = -\int\frac{1}{r}\left(\frac{\partial\phi}{\partial n} + \frac{1}{a_o}M_n\frac{\partial\phi}{\partial\tau_y}\right)\delta(f)\delta(g)\,\mathrm{d}\mathbf{y}\,\mathrm{d}\tau$$

$$- \frac{1}{a_o}\frac{\partial}{\partial t}\int\frac{1}{r}M_n\phi\delta(f)\delta(g)\,\mathrm{d}\mathbf{y}\,\mathrm{d}\tau - \frac{\partial}{\partial x_i}\int\frac{\phi}{r}\hat{n}_i\delta(f)\delta(g)\,\mathrm{d}\mathbf{y}\,\mathrm{d}\tau$$

$$+ H(f)\frac{\partial^2}{\partial x_i\partial x_j}\int\frac{T_{ij}}{r}\delta(g)\,\mathrm{d}\mathbf{y}\,\mathrm{d}\tau \tag{8}$$

The divergence operator can be converted to a temporal derivative in the source time [see Eq. (15) in Ref. 6]. This leads to

$$4\pi\phi(\boldsymbol{x}, t) = -\int\frac{1}{r}\left(\frac{\partial\phi}{\partial n} + \frac{1}{a_o}M_n\frac{\partial\phi}{\partial\tau_y}\right)\delta(f)\delta(g)\,\mathrm{d}\mathbf{y}\,\mathrm{d}\tau$$

$$+ \int\frac{1}{r^2}\phi\cos\theta\,\delta(f)\delta(g)\,\mathrm{d}\mathbf{y}\,\mathrm{d}\tau$$

$$+ \frac{1}{a_o}\frac{\partial}{\partial t}\int\frac{1}{r}[(\cos\theta - M_n)\phi]\delta(f)\delta(g)\,\mathrm{d}\mathbf{y}\,\mathrm{d}\tau$$

$$+ H(f)\frac{\partial^2}{\partial x_i\partial x_j}\int\frac{T_{ij}}{r}\delta(g)\,\mathrm{d}\mathbf{y}\,\mathrm{d}\tau \tag{9}$$

where $\cos\theta = \hat{\boldsymbol{n}}\cdot\hat{\boldsymbol{r}}$. The temporal derivative in observer time of the third integral leaves this equation unattractive for use in numerical applications. Thus, it is desirable to transform this derivative to source time and to bring it inside the integral. First let the Kirchhoff surface S be described by surface coordinates (u^1, u^2), and

let $u^3 = f$. Because of the volume integral in Eq. (9), the mapping $(u^1, u^2, u^3) \rightarrow \boldsymbol{y}$ must exist in the region of nonzero T_{ij}. Let the mapping be a differential function of source time τ. To evaluate the integrals, we first transform $\boldsymbol{y}$ to (u^1, u^2, u^3), and then τ is transformed to g. The Jacobians of the transformations are 1 and $1/(1-M_r)$, where $M_r = v_i \hat{r}_i / a_o$, and $v_i = \partial y_i / \partial \tau$ with (u^1, u^2, u^3) fixed. Integration over $\boldsymbol{u}$ and g gives

$$
\begin{aligned}
4\pi\phi(\boldsymbol{x}, t) &= \int_{D(S)} \left[-\frac{1}{r(1-M_r)} \left(\frac{\partial \phi}{\partial n} + \frac{1}{a_o} M_n \frac{\partial \phi}{\partial \tau_y} \right) \sqrt{g_{(2)}} \right]_{\tau^*} \mathrm{d}u^1\, \mathrm{d}u^2 \\
&+ \int_{D(S)} \left[\frac{\phi \cos\theta}{r^2(1-M_r)} \sqrt{g_{(2)}} \right]_{\tau^*} \mathrm{d}u^1\, \mathrm{d}u^2 \\
&+ \int_{D(S)} \left\{ \frac{1}{a_o r(1-M_r)} \frac{\partial}{\partial \tau} \left[\frac{(\cos\theta - M_n)\phi}{(1-M_r)} \sqrt{g_{(2)}} \right] \right\}_{\tau^*} \mathrm{d}u^1\, \mathrm{d}u^2 \\
&+ \int_{f=u^3>0} \left[\frac{1}{r(1-M_r)} \frac{\partial^2 T_{ij}}{\partial u^i \partial u^j} \right]_{\tau^*} \mathrm{d}u^1\, \mathrm{d}u^2\, \mathrm{d}u^3 \qquad (10)
\end{aligned}
$$

The determinant of the coefficients of the first fundamental form on the surface S is $g_{(2)} = g_{11}g_{22} - g_{12}^2$, where g_{ij} are the metric tensor components for $(i, j = 1, 2)$; see Ref. 13 for details. The term $g_{(2)}$ is a function of $\boldsymbol{u}$ and the source time τ. The surface integrals are over $D(S)$, the domain of S in the space defined by (u^1, u^2). Subscript τ^* indicates evaluation of the integrands at the emission time τ^*, which is the root of

$$
g = \tau - t + \frac{|\boldsymbol{x} - \boldsymbol{y}(u^1, u^2, u^3, \tau)|}{a_o} = 0 \qquad (11)
$$

If the frame velocity is subsonic at the surface and in the region on nonzero T_{ij}, then Eq. (11) has a unique solution. However, Eq. (10) is still valid for supersonically moving surfaces. Farassat and Myers[14] have developed a means of dealing with the singularities caused when $(1 - M_r) \rightarrow 0$. Farassat and Myers[6] evaluated the time derivative in the third integral of Eq. (10) analytically to cast the integral in a form that is useful in numerical applications. Their notation is used here for the moving-surface version of the modified Kirchhoff formula:

$$
\begin{aligned}
4\pi\phi(\boldsymbol{x}, t) &= \int_{D(S)} \left[\frac{E_1 \sqrt{g_{(2)}}}{r(1-M_r)} \right]_{\tau^*} \mathrm{d}u^1\, \mathrm{d}u^2 \\
&+ \int_{D(S)} \left[\frac{\phi E_2 \sqrt{g_{(2)}}}{r^2(1-M_r)} \right]_{\tau^*} \mathrm{d}u^1\, \mathrm{d}u^2 \\
&+ \int_{f=u^3>0} \left[\frac{1}{r(1-M_r)} \frac{\partial^2 T_{ij}}{\partial y_i \partial y_j} \right]_{\tau^*} \mathrm{d}u^1\, \mathrm{d}u^2\, \mathrm{d}u^3 \qquad (12)
\end{aligned}
$$

where

$$
\begin{aligned}
E_1 &= (M_n^2 - 1)\frac{\partial \phi}{\partial n} + M_n \boldsymbol{M}_t \cdot \nabla_2 \phi - \frac{M_n}{a_o} \dot{p} \\
&+ \frac{1}{a_o(1-M_r)^2} [\dot{M}_r (\cos\theta - M_n)\phi] \\
&+ \frac{1}{a_o(1-M_r)} [(\dot{n}_r - \dot{M}_n - \dot{n}_M)\phi \\
&+ (\cos\theta - M_n)\dot{\phi} + (\cos\theta - M_n)\phi\dot{\sigma}]
\end{aligned}
$$

$$
E_2 = \frac{(1-M^2)}{(1-M_r)^2}(\cos\theta - M_n)
$$

Here $\boldsymbol{M}_t$ is the Mach number vector tangent to the surface, and ∇_2 is the surface gradient operator. Also [a dot indicates a source time derivative, with (u^1, u^2, u^3) kept fixed]

$$
\dot{M}_r = \dot{M}_i \hat{r}_i, \qquad \dot{n}_r = \dot{n}_i \hat{r}_i, \qquad \dot{M}_n = \dot{M}_i \hat{n}_i
$$

$$
\dot{n}_M = \dot{n}_i M_i, \qquad \dot{\sigma} = [1/\sqrt{g_{(2)}}]\partial \sqrt{g_{(2)}}/\partial \tau
$$

The convective derivative $\dot{\phi}$ is defined by

$$
\dot{\phi} = a_o M_n \left(\frac{\partial \phi}{\partial n} \right) + a_o \boldsymbol{M}_t \cdot \nabla_2 \phi + \left(\frac{\partial \phi}{\partial \tau_y} \right)
$$

The form of Eq. (12) and E_1 and E_2 were given by Farassat and Myers.[6] The term E_2 was presented in the simplified form shown here by Myers and Hausmann.[15] However, these authors were concerned with solutions to the linear, homogeneous wave equation. Here the dependent variable is restricted to $\phi = a_o^2 \rho'$. Because the governing equation, Eq. (1), was shown to be equivalent to a permeable-surface form of the Ffowcs Williams–Hawkings equation, this restriction accounts for nonlinearities at the Kirchhoff surface. Nonlinear sound generation outside of the Kirchhoff surface is included in the volume integral of quadrupoles in Eq. (12). Through the use of Fourier transforms, Eq. (12) can also be expressed in the frequency domain. This formulation and some of the development shown earlier were presented by Pilon.[16]

At this point, some mention should be made regarding the similarities between Eq. (12) and other solutions to the Ffowcs Williams–Hawkings equation.[3] Di Francescantonio[7] has presented a permeable-surface formulation of the Ffowcs Williams–Hawkings equation that he refers to as the Kirchhoff–FWH equation. Brentner and Farassat[8] have also derived a permeable-surface formulation. They showed that, for a surface placed in a linear region, the permeable-surface, inviscid Ffowcs Williams–Hawkings formulation is equivalent to the linear Kirchhoff formulation plus a volume integral of quadrupoles $(\rho u_i u_j)$. The difference between these authors' formulations and that presented here is that the Kirchhoff surface need not be placed in an entirely linear region. The nonlinearities are accounted for in the use of $\phi = a_o^2 \rho'$ as the dependent variable and the volume integral of quadrupoles T_{ij}. We also note that, when the Kirchhoff surface is placed in a linear region, so that $a_o^2(\rho - \rho_o) = p - p_o$, the modified Kirchhoff formulation is equivalent to the traditional Kirchhoff formulation to second order in the velocity perturbations.

III. Volume Integral

Exact Solution

This section deals with exact and approximate solutions to the volume integral in Eq. (12). As presented in Eq. (12), the volume integral is the equivalent to that presented by Lighthill in his original work.[10] However, it is possible to cast this integral in a different form. The new form makes it possible to obtain more accurate predictions from approximations to T_{ij}. In Eq. (9), the volume integral contribution to the overall solution is

$$
4\pi p_v'(\boldsymbol{x}, t) = \frac{\partial^2}{\partial x_i \partial x_j} \int \frac{T_{ij}}{r} \delta(g)\, \mathrm{d}\mathbf{y}\, \mathrm{d}\tau \qquad (13)
$$

Farassat and Brentner[17] showed that the double divergence can be expressed in terms of time derivatives:

$$
\begin{aligned}
\frac{\partial^2}{\partial x_i \partial x_j} \left[\frac{\delta(g)}{r} \right] &= \frac{1}{a_o^2} \frac{\partial^2}{\partial t^2} \left[\frac{\hat{r}_i \hat{r}_j \delta(g)}{r} \right] \\
&+ \frac{1}{a_o} \frac{\partial}{\partial t} \left[\frac{(3\hat{r}_i \hat{r}_j - \delta_{ij})\delta(g)}{r^2} \right] + \frac{(3\hat{r}_i \hat{r}_j - \delta_{ij})\delta(g)}{r^3} \qquad (14)
\end{aligned}
$$

Using the relation $\partial/\partial t|_x = [(1-M_r)^{-1}\partial/\partial \tau|_x]_{\tau^*}$ allows Eq. (13) to be cast in terms of temporal derivatives at the source time:

$$
\begin{aligned}
4\pi p_v'(\boldsymbol{x}, t) &= \frac{1}{a_o^2} \int \left(\frac{1}{(1-M_r)} \frac{\partial}{\partial \tau} \left\{ \frac{1}{(1-M_r)} \frac{\partial}{\partial \tau} \left[\frac{T_{rr}}{r(1-M_r)} \right] \right\} \right)_{\tau^*} \mathrm{d}\mathbf{y} \\
&+ \frac{1}{a_o} \int \left\{ \frac{1}{(1-M_r)} \frac{\partial}{\partial \tau} \left[\frac{3T_{rr} - T_{ii}}{r^2(1-M_r)} \right] \right\}_{\tau^*} \mathrm{d}\mathbf{y} \\
&+ \int \left[\frac{3T_{rr} - T_{ii}}{r^3(1-M_r)} \right]_{\tau^*} \mathrm{d}\mathbf{y} \qquad (15)
\end{aligned}
$$

where $T_{rr} = \hat{r}_i T_{ij} \hat{r}_j$. After derivation and some algebra, Eq. (15) can be expressed as

$$4\pi p'_v(\boldsymbol{x}, t) = \int_{f>0} \left[\frac{B_1}{a_o^2 r (1 - M_r)^3} + \frac{B_2}{a_o r^2 (1 - M_r)^2} + \frac{B_3}{r^3 (1 - M_r)} \right]_{\tau^*} \mathrm{d}V \tag{16}$$

where

$$B_1 = \hat{r}_i \ddot{T}_{ij} \hat{r}_j + \frac{1}{(1 - M_r)} (3\dot{M}_r \dot{T}_{rr} + \ddot{M}_r T_{rr}) + \frac{1}{(1 - M_r)^2} (3\dot{M}_r^2 T_{rr})$$

$$B_2 = 3\hat{r}_i \dot{T}_{ij} \hat{r}_j + \frac{1}{(1 - M_r)} [\dot{M}_r (3T_{rr} - T_{ii}) - T_{ij} (\dot{M}_i \hat{r}_j + \dot{M}_j \hat{r}_i) - \dot{T}_{ii} + \dot{T}_{ij} (M_r \hat{r}_i \hat{r}_j - M_i \hat{r}_j - M_j \hat{r}_i)] + \frac{1}{(1 - M_r)^2} [\dot{T}_{ij} \hat{r}_i \hat{r}_j (M_r^2 - M^2 - 3M_r) - 3T_{ij} \dot{M}_r (M_i \hat{r}_j + M_j \hat{r}_i) + T_{rr} (3\dot{M}_r + 12 M_r \dot{M}_r - M_i \dot{M}_i + 2M\dot{M})] + \frac{1}{(1 - M_r)^3} [4\dot{M}_r T_{rr} (M_r^2 - M^2)]$$

$$B_3 = 3T_{rr} - T_{ii} + \frac{1}{(1 - M_r)} [M_r (9T_{rr} - 2T_{ii}) - 3T_{ij} (M_i \hat{r}_j + M_j \hat{r}_i)] + \frac{1}{(1 - M_r)^2} \{T_{rr} (12M_r^2 - 3M^2) - T_{ii} (M_r^2 - M^2) + T_{ij} [2M_i M_j - 6M_r (M_i \hat{r}_j + M_j \hat{r}_i)]\} + \frac{1}{(1 - M_r)^3} \times \{T_{rr} (M_r^2 - M^2)(9M_r + 3) + T_{ij} (M_r^2 - M^2) \times [1 - 3(M_i \hat{r}_j + M_j \hat{r}_i)]\} + \frac{1}{(1 - M_r)^4} [3T_{rr} (M_r^2 - M^2)]$$

The contribution from B_1 in Eq. (16) is the often-used far-field approximate solution to Lighthill's equation. The terms B_2 and B_3 are important only in the near field and midfield. Their contribution is significant because it allows for acoustic predictions in a region where CFD data are available. A comparison can then be used to validate the surface integral methodology. Brentner[18] has presented a similar volume integral solution based on temporal derivatives for use in rotorcraft acoustics studies.

Source Approximation

Currently, CFD calculations cannot accurately predict the entire source region in some complex flows. See, for example, the supersonic jet calculations of Mankbadi et al.[19] This is due to the large amount of grid points needed to properly resolve acoustic scales. Memory and computational time restrictions make it impractical to use a grid that will resolve acoustic scales over the entire source region. Because of this, it may be necessary to approximate acoustic sources in the region outside of the Kirchhoff surface. For the jet noise studied here, the region of interest is downstream of the Kirchhoff surface. This is depicted in Fig. 1. One means of approximating T_{ij} downstream of the Kirchhoff surface and solving the resulting volume integrals is presented here. The approximation is based on calculations presented by Mitchell et al.[20] and Mankbadi et al.[19]

Through Fourier transformation, T_{ij} can be expressed as

$$T_{ij}(\boldsymbol{y}, \tau) = \frac{1}{2\pi} \int_{-\infty}^{\infty} \hat{T}_{ij}(\boldsymbol{y}, \omega) e^{-i\omega\tau} \, \mathrm{d}\omega$$

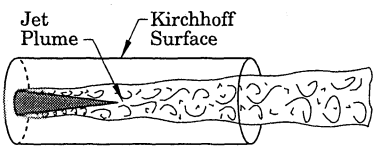

Fig. 1 Jetflow and Kirchhoff surface.

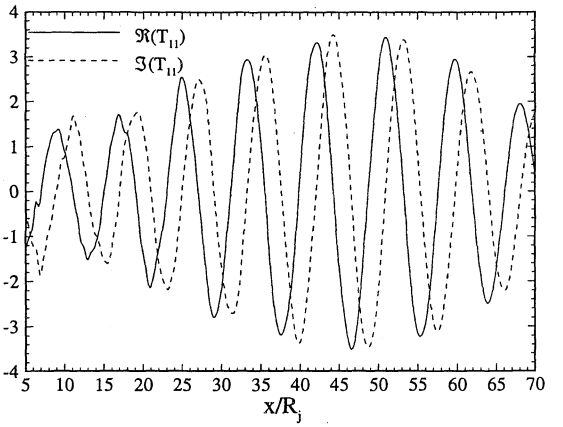

Fig. 2 Centerline axial variations of $\hat{T}_{11}$ at $Sr = 0.20$.

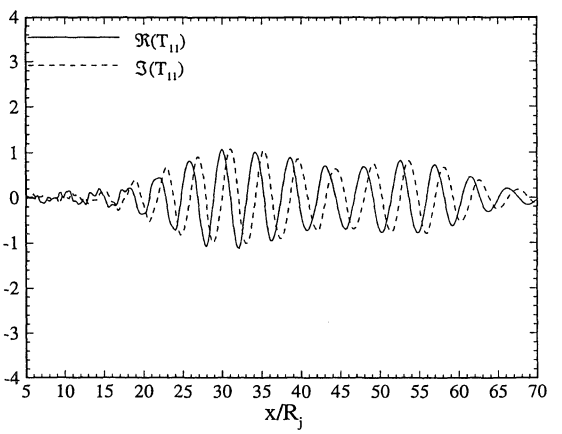

Fig. 3 Centerline axial variations of $\hat{T}_{11}$ at $Sr = 0.40$.

For simplicity, the surface is assumed to be nondeforming and stationary. The emission time τ^* is then uniquely defined, and the effect of the temporal derivatives is simplified considerably. For example,

$$\int_{f>0} \frac{\hat{r}_i \ddot{\hat{T}}_{ij} \hat{r}_j}{a_o^2 r (1 - M_r)^3} \mathrm{d}V = -\frac{1}{2\pi} \int_{-\infty}^{\infty} \frac{\omega^2}{a_o^2} \int_{f>0} \frac{\hat{r}_i \hat{T}_{ij} \hat{r}_j e^{i\omega r/a_o}}{r (1 - M_r)^3} \mathrm{d}\boldsymbol{u} \, \mathrm{d}\omega$$

If enough of the sound production region is contained within the surface, it may be possible to assume that, under simplified conditions, flow disturbances downstream of the Kirchhoff surface have an ordered structure.

This ordered structure can be observed in numerical data made available to the authors. Researchers at NASA Lewis Research Center using the axisymmetric large-scale simulation CFD code of Mankbadi et al.[19,21] based on the 2–4 MacCormack method of Gottlieb and Turkel,[22] simulated an excited, Mach 2.1, cold (jet total temperature = ambient temperature = 294 K), round jet of Reynolds number $Re = 7 \times 10^4$. The jet exit variables were perturbed at a single axisymmetric mode at a Strouhal number of $Sr = 0.20$. The amplitude of the perturbation was 2% of the mean [see Eq. (22) in Ref. 19]. The flow data were converted to the frequency domain at all spatial points using a fast Fourier transform algorithm.[23] Figures 2 and 3 show the axial variation of $\Re(\hat{T}_{11})$ and $\Im(\hat{T}_{11})$ on the jet centerline from 5 to 70 jet radii (the extent of the available data) for the first and second Fourier wave modes, which correspond to $Sr = 0.20$ and 0.40 ($\Re$ and $\Im$ denote the real and imaginary parts, respectively). All variables are normalized by jet nozzle conditions. Higher-order wave modes show similar results. It is evident that

the disturbance amplitude is quite large at the end of the computational domain. Thus, a prediction of the disturbances in the region downstream of the computational domain should be employed.

Mitchell et al.[20] give an approximation to the flow disturbances in the region far downstream of the nozzle in a supersonic, axisymmetric round jet flowfield. This flowfield is similar to the one described earlier, and so their disturbance approximations can also be applied here. The Lighthill stress tensor components are approximated as

$$\hat{T}_{ij}(x_s, r_s; \omega) \simeq \hat{T}_{ij_s}(r_s; \omega) e^{i\kappa(x - x_o)} \tag{17}$$

where $\hat{T}_{ij_s}$ is $\hat{T}_{ij}$ evaluated at the Kirchhoff surface, κ_{ij} is a complex wave number with positive imaginary part, and (x_s, r_s) are cylindrical source coordinates with origin at $(x, r) = (L_k, 0)$. The term κ is assumed to be constant with x, the axial dimension, which corresponds to the surface normal, for the downstream portion of the Kirchhoff surface. Consistent with the preceding approximation of $\hat{T}_{ij}$, the wave number can be defined as

$$\kappa = -i \left. \frac{\partial \hat{T}_{11}/\partial x}{\hat{T}_{11}} \right|_s$$

The positive imaginary part of κ assumes that the disturbance amplitudes are decaying with x downstream of x_o, which is taken as L_k. The assumption of constant κ is reasonable for lower frequencies but breaks down with increasing ω.

If $\hat{T}_{ij}$ is nonzero in a relatively small region outside of the Kirchhoff surface, as was assumed earlier, it is possible to assume a compact source outside of the surface and to approximate the resultant volume integral as [see Eq. (28) in Ref. 19]

$$\hat{p}_v = -\frac{\omega^2}{4\pi\xi a_o^2} \int_{L_k}^{L_v} \int_0^{R_v} \int_0^{2\pi} \left[\cos^2(\vartheta)\hat{T}_{xx} + \sin^2(\vartheta)\cos^2(\varphi)\hat{T}_{rr} \right.$$
$$\left. + \sin(2\vartheta)\cos(\varphi)\hat{T}_{xr} \right] \exp\{i\omega[\xi - (x_s - L_k)\cos(\vartheta)$$
$$- r_s \sin(\vartheta)\cos(\varphi)]/a_o\} r_s \, d\varphi \, dr_s \, dx \tag{18}$$

where $\hat{T}_{xx}$, $\hat{T}_{xr}$, and $\hat{T}_{rr}$ are the stress tensor components converted to cylindrical polar coordinates, ϑ and ξ are the emission angle and radiation distance relative to $(x_s, r_s) = (L_k, 0)$, and φ is the azimuthal angle. Using Eq. (17) in Eq. (18) allows the solution to be written only in terms of surface quantities:

$$\hat{p}_v = -\frac{\omega^2}{4\pi\xi a_o^2} \int_{L_k}^{L_v} \int_0^{R_v} \int_0^{2\pi} \left[\cos^2(\vartheta)\hat{T}_{xx}|_s \right.$$
$$\left. + \sin^2(\vartheta)\cos^2(\varphi)\hat{T}_{rr}|_s + \sin(2\vartheta)\cos(\varphi)\hat{T}_{xr}|_s \right]$$
$$\times \exp(i\{\kappa(x_s - L_k) + \omega[\xi - (x_s - L_k)\cos(\vartheta)$$
$$- r_s \sin(\vartheta)\cos(\varphi)]/a_o\}) r_s \, d\varphi \, dr_s \, dx \tag{19}$$

IV. Test Calculations

To determine the validity of the modified Kirchhoff method, it is necessary to compare known solutions to the governing equations with the results obtained with the Kirchhoff integral. The calculations shown here apply mainly to jet noise predictions, but the preceding derivations remain applicable for general aeroacoustics problems.

A source distribution that resembles that encountered in jet noise predictions can be defined by

$$\hat{T}_{ij} = (\rho uu + \rho uv_r + \rho v_r v_r)_{\max} \exp[i\,\kappa\,|y_1 - y_0| - R/h] \tag{20}$$

where $\hat{T}_{ij}$ is the Fourier transform of T_{ij} and (y_1, R) and (u, v_r) are the near-field source cylindrical coordinates and velocities. Figure 4 shows the relative amplitudes of the components of $\hat{T}_{ij}$ on the centerline ($R = 0$). Here, $\kappa = (5.47 + i\,2.28)/\lambda$. The radiated sound due to this source distribution can be determined through a numerical evaluation of Lighthill's equation. The volume integration is not a burden so long as only one frequency, ω_o, is considered. The dimensions of the volume integration with respect to the cylindrical Kirchhoff surface are shown in Fig. 5. The angular frequency

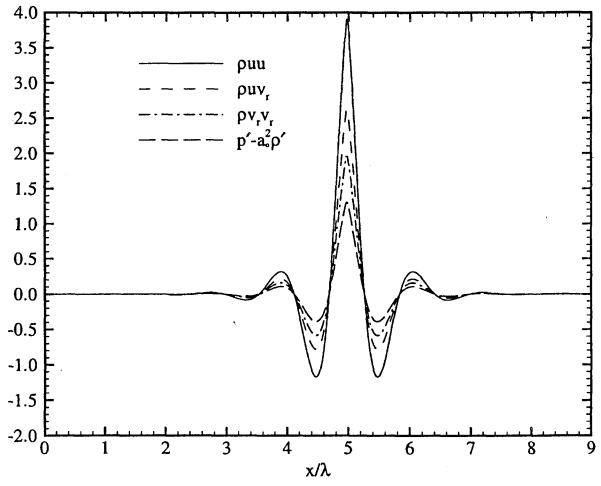

Fig. 4 Centerline amplitude of $\hat{T}_{ij}$ calculated with Eq. (20).

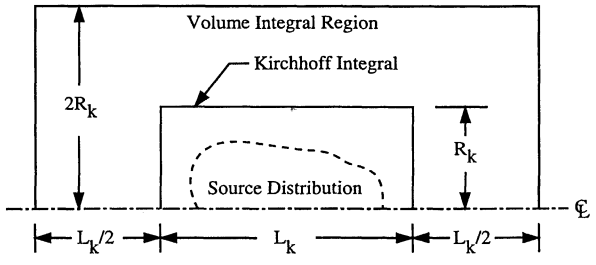

Fig. 5 Surface and volume integral dimensions.

of the source distribution and radiated sound, ω_o, is chosen to correspond to the forcing frequency of a jet simulated previously by the authors.[4] The terms y_o and h are set to 4.95 λ and 0.077 λ, respectively. The source distribution and observer are assumed to be stationary, so that $M = 0$.

The source distribution described earlier was used to validate the various Kirchhoff integral formulations. If the entire source region is enclosed within the Kirchhoff surface, then Eq. (12), without the volume integral, should be able to completely predict the sound radiated to the far field. If the surface is placed in a linear region, then the acoustic variable ϕ can be set to p' as well. Otherwise, ϕ should be set to $a_o^2\rho'$ and the volume integral approximated as necessary. The Kirchhoff surface was a cylinder of radius $R_k = 1.53\,\lambda$. The surface length was varied from $L_k = 9.95\,\lambda$ to $5.51\,\lambda$. When the shorter surface was used, a significant amount of the source distribution remained outside of the surface. The Kirchhoff surfaces were discretized with 40 and 90 uniformly spaced points in the radial and azimuthal directions. The longer and shorter surfaces had 130 and 72 equally spaced points, respectively, in the axial direction. These values were chosen so that the order of accuracy in the numerical quadrature had little effect on the calculated signals. Midpanel first-order quadrature[24] was used to evaluate the integrals numerically. Higher-order quadrature schemes with "enrichment"[25] have been programmed, but the numerical scheme used was determined to be sufficient to validate the developments here.

Figure 6 shows predicted and exact acoustic signals at $(x_1, R) = (15.31\,\lambda, 15.31\,\lambda)$. The signals are normalized by the maximum disturbance amplitude (of the exact signal) at the observation point. Figure 7 shows predicted and exact acoustic signals at $(x_1, R) = (10.41\,\lambda, 1.38\,\lambda)$. Both Figs. 6 and 7 show the signals produced with several levels of approximation. It is apparent that the long Kirchhoff surface can determine the radiated sound with very little error. Open surfaces (those with the downstream end omitted), however, cannot adequately predict radiated noise when the observation point is located downstream of the surface. The shorter surface also accurately determines the sound, as long as the exact volume integral is used outside of the Kirchhoff surface. However, the shorter surface alone, with $a_o^2\rho'$ or p' as the acoustic variable, cannot adequately determine the radiated sound. This is due to the omission of sources outside of

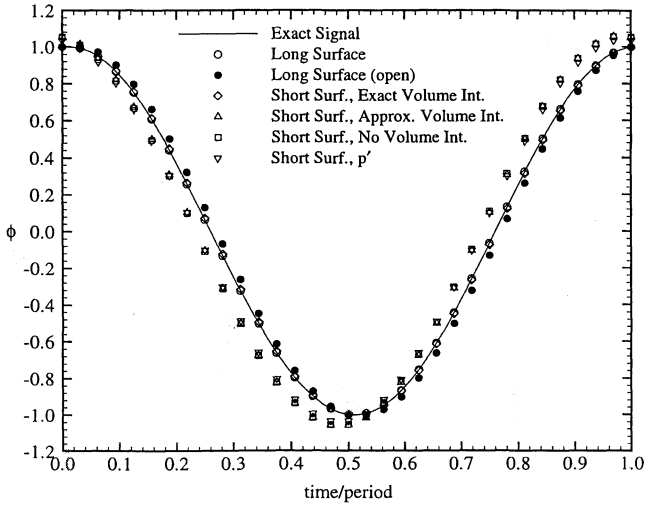

Fig. 6 Predicted and exact acoustic signals at $(x_1, R) = (15.31\lambda, 15.31\lambda)$.

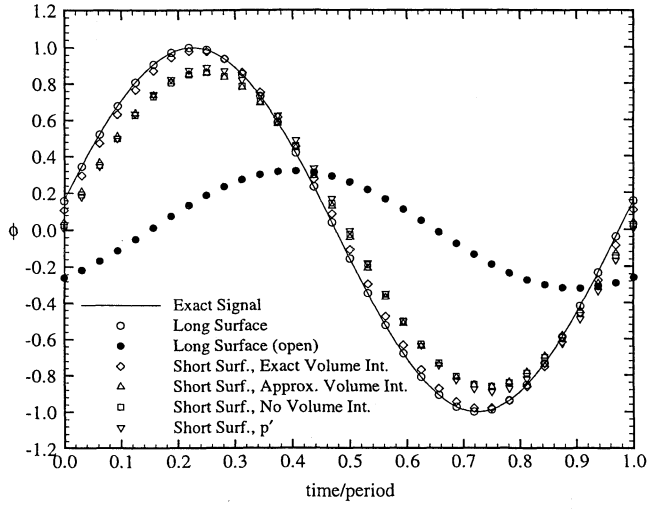

Fig. 7 Predicted and exact acoustic signals at $(x_1, R) = (10.41\lambda, 1.38\lambda)$.

the surface. In this case, the use of the approximate volume integral, Eq. (19), does not significantly improve the accuracy of the acoustic prediction. It is also not apparent whether the use of $a_o^2\rho'$ instead of p' as an acoustic variable represents an improvement. This is most likely due to the nature of the particular source distribution used. A more realistic source distribution would be more broadband, with the separate components of T_{ij} out of phase.

V. Jet Noise Calculations

The CFD calculations discussed in Sec. III were used to predict ϕ, T_{ij}, and the necessary derivatives on similar Kirchhoff surfaces. The surfaces were chosen to match lines in the mesh used for the CFD calculations, so that $L_k = 64.67R_j$ or $59.67R_j$ and $R_k = 8.56R_j$. These values were deemed to be the best choices among the available data, based on mesh spacing and the linearity of disturbances near the surface. (The surfaces extend axially from $x = 5R_j$ to $69.67R_j$ or $64.67R_j$.) However, it is evident from Fig. 2 that the disturbance amplitudes are still quite large at the downstream ends of the surfaces, and so a much longer Kirchhoff surface would be preferable. However, extension of the near-field CFD calculations in the axial direction to generate additional surface data would lead to prohibitive memory requirements. The longer surface used here is probably the shortest permissible for this particular case. The shorter surface is used only for comparison. There were 389 or 359 axial, 167 radial, and 90 azimuthal quadrature points on the Kirchhoff surface. The radial mesh is exponentially stretched about $R = R_j$. Midpoint quadrature was again used in the numerical evaluation of the integrals.

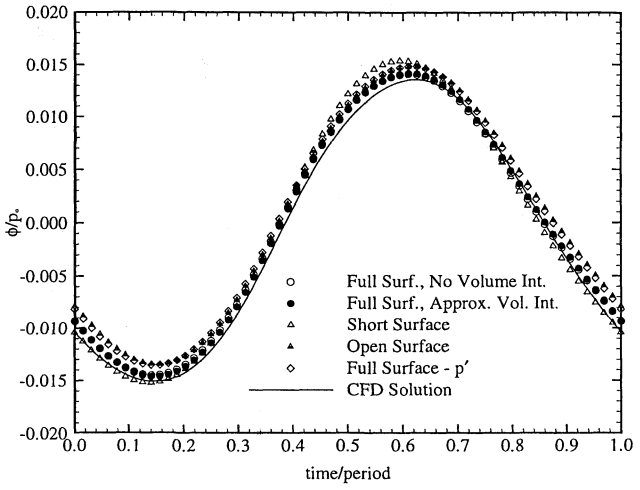

Fig. 8 Predicted acoustic signals at $(x, R) = (33.17R_j, 9.18R_j)$.

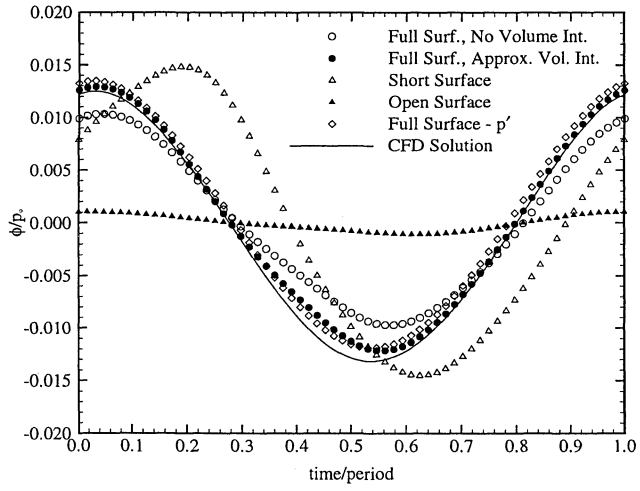

Fig. 9 Predicted acoustic signals at $(x, R) = (70.0R_j, 5.0R_j)$.

Figure 8 shows the acoustic signals, predicted with different levels of approximation on the different Kirchhoff surfaces, at $(x, R) = (33.17\,R_j, 9.18\,R_j)$. Because of restrictions imposed by the number of quadrature points required per acoustic wavelength, only the first four Fourier modes were used in the calculations. All levels of approximation match the signal generated from the first four modes of the CFD calculation reasonably well at this observation point. The best predictions are obtained with the full Kirchhoff surface. An open surface, i.e., one without the downstream end included, was also used. Many researchers have ignored nonlinearities caused by flow through the surface in this manner. The omission of this portion of the surface has a small but noticeable effect at this observation point. Figure 9 shows acoustic signals at $(x, R) = (70.0\,R_j, 5.0\,R_j)$. Here it is evident that the shorter surface, while omitting only $5R_j$ from the length of the surface, produces an unacceptable prediction. It is also clear that open-surface Kirchhoff methods (e.g., Refs. 20 and 26) are not appropriate acoustic prediction tools when the observation point lies downstream of the surface and close to the jet axis.

The approximate volume integral presented in Eq. (19) again provides little improvement over the prediction obtained with the full Kirchhoff surface. Because this observation point is just downstream of the Kirchhoff surface and is in a nonlinear disturbance region, the use of some approximate volume integral is necessary to produce an adequate prediction. Although the approximate integral presented here appears to be ineffective, the methodology employed could be useful in future predictions. In this region, the use of p' leads to a similarly accurate prediction. However, the authors feel, based on the development presented in Sec. II, that the use of $\phi = a_o^2\rho'$ will allow for more accurate predictions at most observer points. It would

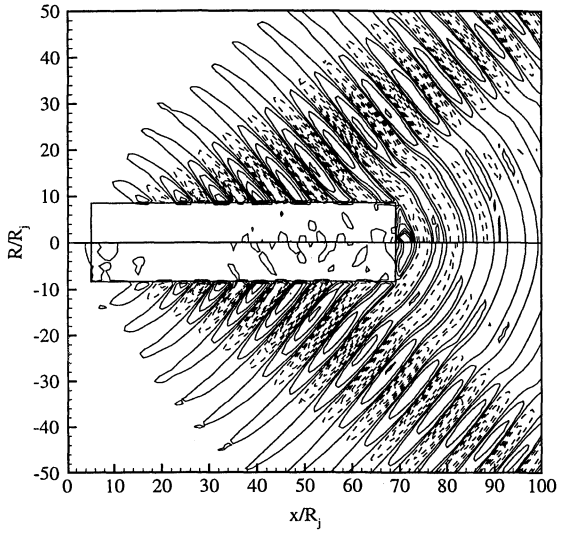

Fig. 10 Instantaneous perturbation contours (normalized by free-stream pressure). Contours: min = −0.025, max = 0.025, and increment = 0.005. Negative contours are dashed; $R > 0$, $\phi = a_o^2\rho'$, and $R < 0$, $\phi = p'$.

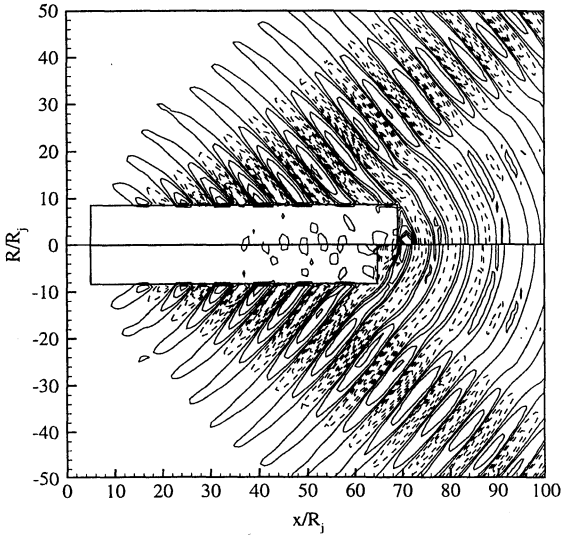

Fig. 11 Instantaneous perturbation contours (normalized by free-stream pressure). Contours: min = −0.025, max = 0.025, and increment = 0.005. Negative contours are dashed; $\phi = a_o^2\rho'$; $R > 0$, $L_k = 65R_j$, and $R < 0$, $L_k = 60R_j$.

be beneficial to extend the near-field CFD calculations farther into the far field so that more valid comparisons could be made.

Figure 10 shows instantaneous contours of ϕ/p_o in the near and mid acoustic fields. The contours shown above the centerline were calculated using $a_o^2\rho'$ as the acoustic variable, whereas those below the centerline were calculated with $\phi = p'$. The volume integral was omitted in both cases. Both prediction methods show similar radiation patterns and appear to capture the Mach wave radiation in the region $R > 10R_j$. The spherical radiation downstream of the Kirchhoff surface is predicted with both variables, but the contours of $a_o^2\rho'$ are greater in magnitude than those of p'.

Figure 11 shows instantaneous contours of $a_o^2\rho'$ in the near and mid acoustic fields. The contours shown above the centerline were calculated using the Kirchhoff method on the longer surface, whereas those below the centerline were calculated with the shorter Kirchhoff surface. No volume integral approximations were utilized. Both predictions again show the Mach wave radiation. Both surfaces also predict radiation downstream of the surface ends. The radiation appears to emanate from an equivalent source located on the jet axis around $x_s R_j$. The downstream radiation predictions are slightly out of phase due to the omission of sources inside the shorter Kirchhoff surface. To ease this error, it is necessary to utilize a

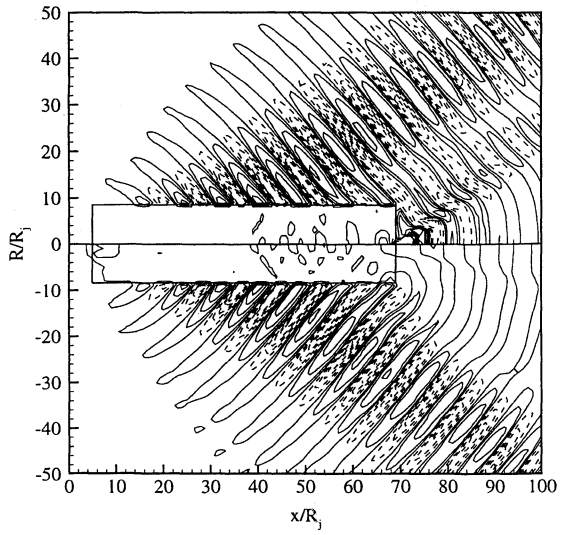

Fig. 12 Instantaneous perturbation contours (normalized by free-stream pressure). Contours: min = −0.025, max = 0.025, and increment = 0.005. Negative contours are dashed; $\phi = a_o^2\rho'$; $R > 0$, approximate volume integral, and $R < 0$, open Kirchhoff surface.

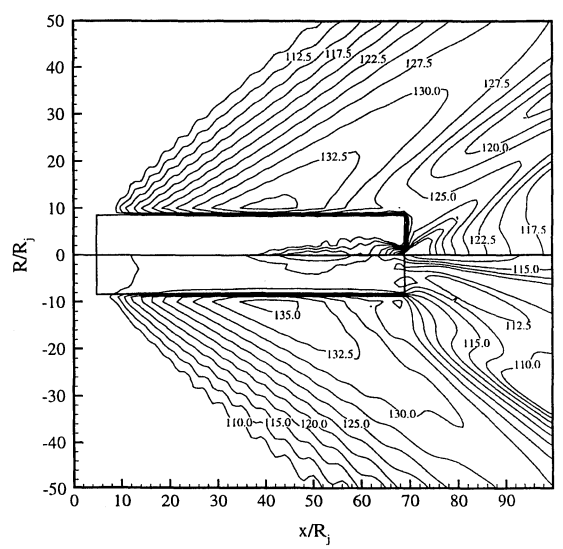

Fig. 13 Sound pressure level (*Re*: 20 μPa) contours; $\phi = a_o^2\rho'$; $R > 0$, approximate volume integral, and $R < 0$, open Kirchhoff surface.

Kirchhoff surface that is as long as possible. However, the near-field CFD predictions must retain their accuracy on the Kirchhoff surface.

Instantaneous perturbation contours are again shown in Fig. 12. The contours shown above the jet axis were calculated using the longer Kirchhoff surface and the volume integral approximation. For comparison, the contours shown below the centerline were calculated with an open Kirchhoff surface. There is a large zone of relative silence downstream of the open Kirchhoff surface caused by the omission of sound that propagates through the downstream portion of the surface. The approximate volume integral, Eq. (19), predicts large-amplitude disturbances near the end of the Kirchhoff surface. This is due to the far-field nature of the approximation. For observer locations farther away from the surface, the disturbances begin to resemble those emitted from the equivalent source at $x_s R_j$. The effects of the use of the Kirchhoff method on a closed surface, as opposed to an open surface, are also shown in Fig. 13, which shows sound pressure level contours calculated with the two methods. The differences between the two predictions are clearly evident in the region downstream of the computational surface. In the region where $R \geq 10R_j$, both methods show qualitative agreement with the results presented by Troutt and McLaughlin[27] and those of Mankbadi et al.[28] (Note that the calculations shown here

were based on an axisymmetric CFD calculation. The experimental data in Ref. 27 are made up of nonaxisymmetric disturbances, so that a direct quantitative comparison is not possible.) However, the open-surface calculation again shows a large zone of silence downstream of the surface, whereas the prediction from the full method (with axisymmetric volume integral approximation) shows a lobe of high intensity near the axis just downstream of the surface. This high-intensity region appears in an area where hydrodynamic disturbances are propagating through and out of the CFD domain. Boundary conditions in the CFD calculations, as well as the large-scale structures existent in the jet flowfield, may be contributing to these large-amplitude predictions. However, the authors feel that the use of the full Kirchhoff integral, with appropriate refraction corrections and approximations to the volume integral, provides the best means of accurately predicting this acoustic field. Clearly, more work is required in the development of these approximations.

VI. Conclusions

Surface integral formulations based on Kirchhoff's integral equation are becoming popular tools in aeroacoustic analysis. Development of an extension to this formulation was presented here. The extension arose from a desire to make the method more applicable to jet noise calculations. The newly derived Kirchhoff approach accounts for noise generation at and outside of the Kirchhoff surface through the use of disturbance density as the acoustic variable. Encouraging results have been shown for model problems related to jet noise prediction, though additional work is required on the volume integral approximations. The method should also be applicable to other types of aeroacoustics problems where Kirchhoff methods are employed. Inclusion of an additional correction to account for refractive effects outside of the surface will improve prediction accuracy. These additional corrections will be developed in the future.

Acknowledgments

This research was supported in part by Grant ASC950019P from the Pittsburgh Supercomputing Center, sponsored by the National Science Foundation. This work was sponsored by NASA Langley Research Center under Grant NAG 1-1660. Kristine Meadows served as the Technical Monitor. Feri Farassat of NASA Langley Research Center also provided insight and valuable assistance with the theoretical development in this work.

References

[1]Kirchhoff, G. R., "Zur Theorie der Lichtstrahlen," *Annalen der Physik und Chemie*, Vol. 18, 1883, pp. 663–695.

[2]Lyrintzis, A. S., "Review, The Use of Kirchhoff's Method in Computational Aeroacoustics," *Journal of Fluids Engineering*, Vol. 116, Dec. 1994, pp. 665–676.

[3]Ffowcs Williams, J. E., and Hawkings, D. L., "Sound Generation by Turbulence and Surfaces in Arbitrary Motion," *Philosophical Transactions of the Royal Society of London*, Vol. 264A, May 1969, pp. 321–342.

[4]Pilon, A. R., and Lyrintzis, A. S., "An Improved Kirchhoff Method for Jet Aeroacoustics," AIAA Paper 96-1709, May 1996.

[5]Pilon, A. R., and Lyrintzis, A. S., "Surface Integral Methods for Computational Aeroacoustics," AIAA Paper 97-0020, Jan. 1997.

[6]Farassat, F., and Myers, M. K., "Extension of Kirchhoff's Formula to Radiation from Moving Surfaces," *Journal of Sound and Vibration*, Vol. 123, No. 3, 1988, pp. 451–460.

[7]Di Francescantonio, P., "A New Boundary Integral Formulation for the Prediction of Sound Vibration," *Journal of Sound and Vibration*, Vol. 202, No. 4, 1997, pp. 491–509.

[8]Brentner, K. S., and Farassat, F., "An Analytical Comparison of the Acoustic Analogy and Kirchhoff Formulations for Moving Surfaces," *Proceedings of the American Helicopter Society 53rd Annual Forum*, Vol. 1, American Helicopter Society, Alexandria, VA, 1997, pp. 687–696.

[9]Crighton, D. G., Dowling, A. P., Ffowcs Williams, J. E., Heckl, M., and Leppington, F. G., *Modern Methods in Analytical Acoustics: Lecture Notes*, Springer–Verlag, London, 1992, pp. 334–342.

[10]Lighthill, M. J., "On Sound Generated Aerodynamically, I. General Theory," *Proceedings of the Royal Society of London*, Vol. A211, March 1952, pp. 564–587.

[11]Farassat, F., "Introduction to Generalized Functions with Applications in Aerodynamics and Aeroacoustics," NASA TP-3428, May 1994.

[12]Farassat, F., "Discontinuities in Aerodynamics and Aeroacoustics: The Concept and Applications of Generalized Functions," *Journal of Sound and Vibration*, Vol. 55, No. 2, 1977, pp. 165–193.

[13]Aris, R., *Vectors, Tensors and the Basic Equations of Fluid Mechanics*, Dover, New York, 1962, Chap. 9.

[14]Farassat, F., and Myers, M. K., "The Kirchhoff Formula for a Supersonically Moving Surface," *Proceedings of the CEAS/AIAA 1st Joint Aeroacoustics Conference (AIAA 16th Aeroacoustics Conference)*, Vol. 1, DGLR, Bonn, Germany, 1995, pp. 475–480 (CEAS/AIAA Paper 95-062).

[15]Myers, M. K., and Hausmann, J. S., "On the Application of the Kirchhoff Formula for Moving Surfaces," *Journal of Sound and Vibration*, Vol. 139, No. 1, 1990, pp. 174–178.

[16]Pilon, A. R., "Development of Improved Surface Integral Methods for Jet Aeroacoustic Predictions," Ph.D. Thesis, Dept. of Aerospace Engineering and Mechanics, Univ. of Minnesota, Minneapolis, MN, Jan. 1997.

[17]Farassat, F., and Brentner, K. S., "The Uses and Abuses of the Acoustic Analogy in Helicopter Rotor Noise Prediction," *Journal of the American Helicopter Society*, Vol. 33, No. 1, 1988, pp. 29–36.

[18]Brentner, K. S., "An Efficient and Robust Method for Predicting Rotor High-Speed Impulsive Noise," AIAA Paper 96-0151, Jan. 1996.

[19]Mankbadi, R. R., Hayder, M. E., and Povinelli, L. A., "Structure of Supersonic Jet Flow and Its Radiated Sound," *AIAA Journal*, Vol. 32, No. 5, 1994, pp. 897–906.

[20]Mitchell, B. E., Lele, S. K., and Moin, P., "Direct Computation of the Sound Generated by Subsonic and Supersonic Axisymmetric Jets," Thermosciences Div., Dept. of Mechanical Engineering, Research Rept. TF-66, Stanford Univ., Stanford, CA, Nov. 1995.

[21]Mankbadi, R. R., Shih, S. H., Hixon, R., and Povinelli, L. A., "Direct Computation of Sound Radiation by Jet Flow Using Large-Scale Equations," AIAA Paper 95-0680, Jan. 1995.

[22]Gottlieb, D., and Turkel, E., "Dissipative Two-Four Methods for Time-Dependant Problems," *Mathematics of Computation*, Vol. 30, No. 136, 1976, pp. 703–723.

[23]Press, W. H., Teukolsky, S. A., Vetterling, W. T., and Flannery, B. P., *Numerical Recipes in Fortran: The Art of Scientific Computing*, Cambridge Univ. Press, Cambridge, England, UK, 1992, Chap. 12.

[24]Brentner, K. S., "Numerical Algorithms for Acoustic Integrals—The Devil is in the Details," AIAA Paper 96-1706, May 1996.

[25]Meadows, K. R., and Atkins, H. L., "Towards a Highly Accurate Implementation of the Kirchhoff Approach for Computational Aeroacoustics," *Journal of Computational Acoustics*, Vol. 4, No. 2, 1996, pp. 225–241.

[26]Lyrintzis, A. S., and Mankbadi, R. R., "Prediction of the Far-Field Jet Noise Using Kirchhoff's Formulation," *AIAA Journal*, Vol. 34, No. 2, 1996, pp. 413–416.

[27]Troutt, T. R., and McLaughlin, D. K., "Experiments on the Flow and Acoustic Properties of a Moderate-Reynolds-Number Supersonic Jet," *Journal of Fluid Mechanics*, Vol. 116, March 1982, pp. 123–156.

[28]Mankbadi, R. R., Shih, S. H., Hixon, R., Stuart, J. T., and Povinelli, L. A., "Extension of Near Field to Far Field Jet Noise Prediction," AIAA Paper 96-2651, July 1996.

S. Glegg
Associate Editor